Junction Dynamics and the Elasticity of Networks

K. L. Ngai and C. M. Roland*

Naval Research Laboratory, Washington, D.C. 20375-5342

Received July 2, 1993; Revised Manuscript Received February 7, 1994®

ABSTRACT: The restrictions on the configurations available to the cross-link junctions of a network, arising from its presence in a dense phase, have a well-established effect on the mechanical properties of elastomers. These constraints give rise to intermolecular cooperativity of the junction motions and hence can be well described by models of constraint dynamics in relaxation phenomena. This connection between junction dynamics and elasticity of networks is illustrated by comparing the predictions of the coupling model of relaxation with the constrained junction model of Flory. The comparison is borne out by recent ^{31}P NMR results on networks.

Introduction

Mechanical Equilibrium. Both the topology and the motion of chain molecules are governed by the same intramolecular and intermolecular potentials and correlations; nevertheless, theoretical and experimental studies invariably are restricted to one or the other of these fundamental aspects of polymer behavior. Elastomers (i.e., cross-linked rubber) offer an important advantage to such investigations because the material can be studied in mechanical equilibrium and many theories address the elastic behavior of networks of chain molecules. Indeed, this is an obvious starting point for any attempt to account for the general deformation behavior of polymers.

The force required to distend a sufficiently long (ca. 100 backbone bonds) flexible chain is directly proportional to the displacement, at least when the resulting end-to-end distance does not approach the contour length of the chain. The nature of the intermolecular interactions does not modify this Gaussian behavior as long as such interactions are independent of the chain configuration. Calculation of the stress–strain relationship for a real network requires analysis of the response of a given chain to the imposition of a bulk deformation, described classically by two extremes, the phantom and the affine model.

The cross-link sites in a real network are embedded in a high concentration of neighboring chain segments. At typical cross-link densities, spatially neighboring junctions are not topological neighbors; that is, the volume existing between a directly connected pair of junctions will contain many other junctions. Such an interpenetration of network cross-link points suggests an affine response, whereby the network deforms as a continuum in which the cross-link points are embedded, the displacement of each pair of junctions from their initial end-to-end separation being proportional to the macroscopic displacement. For an affine network, the retractive force for simple extension is given by[1]

$$f_{aff} = (NRT/L_0)(V/V_0)^{1/3}f(\lambda) \quad (1)$$

with

$$f(\lambda) = \lambda - \lambda^{-2} \quad (2)$$

where λ is the extension ratio, N is the number of elastically effective network chains in the volume, V, RT has its usual significance, and L_0 and V_0 are the length and volume in the reference state defined as that in which the chains have their unperturbed configuration.

Even in the absence of diluent, the concept of junctions as firmly embedded as required by the affine model is inconsistent with the large free volume available to chain segments in the elastomeric state and the thermal agitation they experience. The other extreme of rubber elasticity theories employs the concept of volumeless chains able to freely pass through one another. Although the average displacement of such phantom network strands remains proportional to the macroscopic strain, Brownian motion of the junctions enables their diffusion significant distances from an end-to-end separation characterized by affine displacement. The elastic force for a perfect (no dangling ends) network of phantom chains is[2,3]

$$f_{ph} = (1 - 2/\phi)(NRT/L_0)(V/V_0)^{-1/3}f(\lambda) \quad (3)$$

where ϕ is the junction functionality and $2N/\phi V$ is the cross-link density. The freedom to rearrange configurations reduces the displacement of chains, and hence the equilibrium stress, from that of affinely deforming junctions (by half for tetrafunctional cross-links).

Real networks exhibit a strain dependence of their elastic stress that is at variance with the predictions of either the affine or the phantom network models. This is unsurprising since the junctions in a real polymer network fluctuate away from positions corresponding to affine displacement, while interferences from neighboring chains reduce the magnitude of such fluctuations from that available to a phantom network.[4,5] In the constrained junction model of Flory and co-workers,[6-8] the fluctuation of the junctions is limited to a domain of constraints imposed by steric hindrances from neighboring segments, with the range and position of these domains changing with deformation. Flory introduced the parameter κ, defined in terms of the number of junctions in the volume occupied by a network chain, as a measure of the severity of the local constraints relative to those imposed by the phantom network. The elastic stress in the constrained junction model is given by[5-8]

$$f_c = (1 - 2/\phi)(NRT/L_0)(V/V_0)^{1/3}f(\lambda)(1 + f_c/f_{ph}) \quad (4)$$

where f_c/f_{ph} expresses the ratio of the contribution to the stress from local constraints on junction fluctuations to that for phantom chains. The contribution to the force from the constraints is zero for $\kappa = 0$, while for a perfect network

® Abstract published in *Advance ACS Abstracts*, March 15, 1994.

$$\lim_{\kappa \to \infty} f_c/f_{ph} = \frac{2}{\phi - 2} \tag{5}$$

In general, the quantity f_c/f_{ph} can be obtained by numerical evaluation of free energy integrals involving functions of the strain[8,9] or more usually evaluated experimentally. Equation 4 bears a resemblance to the empirical Mooney–Rivlin expression[3]

$$f_{MR} = (V/V_0)^{1/3} f(\lambda)(2C_1 + 2C_2\lambda^{-1}) \tag{6}$$

which adequately describes experimental data in uniaxial extension. The C_1 elastic constant is identifiable with the number of network chains, and the ratio C_2/C_1 can be taken as a measure of the relative magnitude of the constraints on junction fluctuations.

Recent molecular dynamics simulations[10] have demonstrated the existence of local constraints on the network junctions, even for strand lengths less than the molecular weight necessary for chain entanglements. Rubber elasticity models other than Flory's have been developed, with various ideas advanced to describe the topological constraints on a network and their effect on its mechanical response.[11-19] While in the Flory theory the constraints on the network fluctuations are considered to exist specifically at the cross-link sites, a modification of the constrained junction model is the constrained chain theory,[19] in which constraints from neighboring chains act along the entire chain.

Polymer Dynamics. The picture that emerges from current rubber elasticity theory is one of chains frustrated by intermolecular constraints in their effort to achieve all the configurations available to an isolated chain. Neutron spin-echo studies provide direct evidence for the existence in real networks of limitations on the cross-link motion, which reduce their range of fluctuations below the phantom network prediction.[20] Clearly, a deeper understanding of network elasticity and firmer corroboration of any model thereof require study of the chain dynamics.

The many modes of motion of flexible macromolecules give rise to a complicated range of length scales encompassing many decades. Moreover, different experimental techniques, sensitive not only to different time scales but also to different chemical moieties, can yield seemingly disparate pictures of the molecular motions of polymers. This situation is further confused by the many different approaches to interpreting these motions. Theories are often at odds with one another, either because of underlying ideas which are mutually contradictory or simply because distinctly different aspects of the dynamics are being considered.

The coupling model[21-23] is an attempt to provide a unifying picture of the constraint dynamics of relaxation phenomena in a dense phase. Motion of any moiety in a dense-packed system is governed by constraints originating from intramolecular and intermolecular interactions with other groups. The essence of the coupling model can be summarized as follows. At short times each moiety relaxes independently, the dynamic constraints not having built up to an extent sufficient to impede the motion. In this short time regime, the relaxation rate W_0 can be expressed in terms of transitions of independent moieties. The correlation function describing the independent relaxation in this short time regime has the exponential form $\exp[-(t/\tau_0)]$, where $\tau_0 \equiv 1/W_0$. As an example, in certain cases it is appropriate to model W_0 as a thermally activated process, i.e.,

$$W_0 = \tau_\infty^{-1} \exp(-E_a/RT) \tag{7}$$

where E_a and τ_∞^{-1} can be identified as an energy barrier and attempt frequency, respectively. However, from general physical principles[21-23] there exists a (temperature-insensitive) time scale, t_c, after which the average relaxation rate of the moieties will be slowed down by the dynamic constraints. It has been found that the averaged relaxation rate $W(t)$ assumes the form[21-23]

$$W(t) = W_0(t/t_c)^{-n}, \quad t > t_c \tag{8}$$

As a consequence, the normalized correlation function that describes the relaxation of a macroscopic variable will have the stretched exponential form

$$C_c(t) = \exp[-(t/\tau^*)^{1-n}], \quad t > t_c \tag{9}$$

where

$$\tau^* = [(1-n)t_c^{-n}\tau_0]^{1/(1-n)} \tag{10}$$

From experimental data of amorphous polymers[23-26] we have previously deduced that t_c has a magnitude lying between 10^{-12} and 10^{-11} s. Recent neutron scattering experiments and computer simulations have provided direct evidence for the existence of a crossover time with this order of magnitude.[27,28]

Particularly for amorphous polymers, the coupling model has provided numerous predictions which have been experimentally verified.[25] In addition, a number of anomalies, otherwise without explanation, have been shown[29] to be a natural consequence of constraint dynamics or intermolecular cooperativity as described by the coupling model. From the demonstrated generality of the model, it is clear that a polymer network is another dense system, the dynamics of which should be well described by the coupling model. The same arguments given by Flory[5-8] for the importance of considering local constraints on junctions (as caused by interactions with neighboring chains) in his treatment of elasticity of polymer networks justify the need to use models, such as the coupling model, which explicitly consider the effect on the dynamics of these constraints when describing junction relaxation.

A purpose of this paper is to extend the coupling model from the realm of polymer dynamics to that of equilibrium mechanical behavior. Specifically, the connections between network theory (viz., Flory constrained junction model) and the coupling model will be discussed. We invoke recent findings[30] on the junction dynamics in polymer networks as measured by ^{31}P nuclear magnetic relaxation (NMR) to show how a connection between the coupling model and the Flory rubber elasticity model is borne out by experimental data. Moreover, by virtue of good agreement with the NMR data, the coupling model can provide physical meaning to the experimental results.

Results

Connections between the Flory Model and the Coupling Model. From the brief reviews of the Flory constrained junction model and the coupling model given above, it is evident that both are concerned with the effects of constraints on junctions in polymer networks. Flory used the constraints on junctions to model the effects of restrictions on the fluctuations of network junctions imposed by neighboring chains, deriving an expression for the modification of the elastic stress for a perfect network of phantom chains. Analogously, the coupling

model (when applied to junctions in polymer networks) uses the dynamics of the constraints on junctions to model the slowing down of the motions of the network junctions caused by interactions with neighboring chains and thus obtain the modification of the correlation function of relaxation of junctions for a perfect network of phantom chains, $C_{ph}(t)$. Thus, the Flory and the coupling models address different manifestations of the same physical phenomenon—the constraints on network junctions imposed by the surrounding chains. Flory was concerned with the consequent restriction on the configurations available to the network, which affects its elastic energy. The coupling model focuses on the manner in which intermolecular constraints retard relaxation. Hence, there is a direct connection between equilibrium mechanical properties and the dynamics underlying stress relaxation. Of course, a connection between random equilibrium fluctuations (in this case of the network junctions) and the manner in which a system dissipates external perturbations (e.g., mechanical stress) is by no means a new idea, representing the central premise of linear response theory.[31]

From the idea that phantom chains are able to freely pass through one another, we expect that $C_{ph}(t)$ has an exponential time dependence, $\exp[-(t/\tau_0)]$, where τ_0 is the time-independent junction relaxation time. At temperatures sufficiently above T_g, τ_0 can be well approximated by the Arrhenius temperature dependence of eq 7, in which E_a is the true microscopic conformational energy barrier to motion of junctions in the phantom network model. Following the general physical principle behind the coupling model, the constraints on junctions will modify $C_{ph}(t)$ to $C_c(t)$ as given by eqs 8 and 9. The coupling parameter, n, determines both the nonexponentiality of the constraints-modified correlation function and the correlation time τ^*. In particular, the temperature dependence of τ^* is modified to

$$\tau^* = \tau_\infty^* \exp[-E_a^*/RT] \tag{11}$$

where

$$\tau_\infty^* = [(1-n)t_c^{-n}\tau_\infty]^{1/(1-n)} \tag{12}$$

and

$$E_a^* = E_a/(1-n) \tag{13}$$

By examining eqs 12 and 13, we see that the degrees of modification of the preexponential and the activation energy, from the phantom network values to the constrained values, are proportional to n. In the coupling model, the magnitude of n increases with the severity of the constraints relative to those imposed by the phantom network. Thus, n bears a similarity to the quantity κ in the constrained junction model. Flory expressed the contribution of constraints to the elasticity of the network by the ratio f_c/f_{ph} (eq 4). Similarly, in the coupling model we may use the logarithm of the ratio

$$\log(\tau_\infty/\tau_\infty^*) = \log\{(1-n)^{-1/(1-n)}(\tau_\infty/t_c)^{-n/(1-n)}\} \tag{14}$$

and the ratio

$$\frac{E_a^*}{E_a} = \frac{1}{1-n} \tag{15}$$

as gauges of modification of the junction relaxation by constraints. Typically τ_∞ is of the 10^{-14} s. This, together with $10^{11} < t_c^{-1} < 5 \times 10^{11}$ s^{-1}, indicates that the ratio τ_∞/t_c is much less than unity. Hence, both $\log(\tau_\infty/\tau_\infty^*)$ and the difference $E_a^*/E_a - 1$ increase with n or the severity of constraints, and both quantities vanish at $n = 0$ (corresponding to a phantom network). These dependencies on n are analogous to the dependence of the quantity f_c in Flory's model.

The proffered analogy is supported by an examination of the dependencies on cross-link density, diluent concentration, cross-link functionality, and macroscopic strain of the junction constraints of the Flory model with n, $\log(\tau/\tau^*)$ and $E_a^*/E_a - 1$ in the coupling model. It is usual practice to normalize the effect of the constraints on the junction fluctuations by some quantity characterizing the phantom network. For example, the parameter κ in the Flory theory is the ratio of the domain of the constraints to that of the fluctuations of the phantom chains. Similarly, while the restoring force arising in the deformed network can be expressed as the sum of the contribution from the phantom chains (i.e., due to network connectivity) and that due to the constraints, the ratio of forces, f_c/f_{ph}, is the parameter usually evaluated in assessing experimental variables. For our purposes, such a normalization in terms of a hypothetical unconstrained network is unnecessary. To consider the dynamics of the network junctions, we focus directly on the junction constraints per se.

The topological structure of a network will influence the degree to which a junction can diffuse about its average position. Higher cross-link densities increase the elastic modulus, thereby decreasing the normalized parameters κ and f_c/f_{ph}. However, the severity of the constraints on junction motion increases with cross-link density.[32] Similarly, an increase in the number of chains emanating from a cross-link site (i.e., larger ϕ) impedes their motion, as reflected in the factor $(1 - 2/\phi)$ difference in the stress of an affine (no junction diffusion) versus a phantom (no intermolecular constraints) network. Certainly dilution is expected to isolate the cross-link sites from the surrounding segments; the consequent reduction of the intermolecular constraints on the junctions has been observed experimentally.[8,33,34] By essentially the same mechanism as dilution, elongation likewise alleviates the restrictions of the junctions from neighboring segments,[8,35-37] in that the "domain" of the constraints extends along the stretch direction. The elastic behavior of networks thus becomes more "phantom-like" at higher elongations, as has long been observed experimentally.

The premise from rubber elasticity theory is that dense packing of chains (unfortunately often referred to as entanglements although the effects are not necessarily equivalent to the long-range topological interactions suggested by this term) gives rise to constraints on the motion of the network junctions. This idea has an obvious correspondence to a model for constrained dynamics such as the coupling model,[21-26] when the latter is specialized to describe the dynamics of network junctions. The principal physical quantity in the coupling model that governs the junction dynamics is the coupling parameter, n, which in turn determines via eqs 14 and 15 the deviations measured by $\log(\tau_\infty/\tau_\infty^*)$ and $E_a^*/E_a - 1$ from phantom network junction dynamics. From any of the theoretical frameworks[21,22] of the coupling model, it emerges that n is proportional to the strength of the intermolecular constraints acting on the junction. Although the coupling parameter characterizes relaxation dynamics, it obviously could be used as well to describe network elasticity, at least in the context of the Flory model. Let us examine

Table 1

network feature	anticipated effect	flory model f_c	coupling model n	coupling model $E_a^*/E_a - 1$	coupling model $\log(\tau_\infty/\tau_\infty^*)$	^{3}P NMR[a] n	^{3}P NMR[a] $E_a^*/E_a - 1$	^{3}P NMR[a] $\log(\tau_\infty/\tau_\infty^*)$
higher cross-link density	more firmly embedded junctions	higher[b]	higher	higher	higher	higher[g]	higher[h]	higher[i]
diluent	reduced severity of constraints	lower[c]	lower	lower	lower	lower[g]	lower[h]	lower[i]
higher cross-link functionality	more constrained junctions	higher[d]	higher	higher	higher			
extension	alleviation of constraints	lower[e]	lower[f]	lower[f]	lower[f]			

[a] Reference 30. [b] Reference 32. [c] References 8 and 34. [d] References 32 and 42. [e] References 8 and 35–37. [f] Tentative (see ref 41). [g] See Figure 1. [h] See Figure 2. [i] See Figure 3.

the dependencies of these quantities on cross-link density, diluent concentration, cross-link functionality, and macroscopic strain. In the following we need to consider only the dependencies of n, since the corresponding dependencies of the other two quantities are immediately determined from that of n through eqs 14 and 15.

From the arguments given before in discussing the Flory model, we may conclude that higher cross-link density and cross-link functionality will enhance the strength of the intermolecular constraints and consequently n. On the other hand, with the addition of diluent the junctions become increasingly isolated from the neighboring chain segments, so that the strength of the intermolecular constraints, and hence n, decreases. Such a decrease of n with diluent concentration, as also seen for the local segmental motion[38] in amorphous polymers and in the terminal motion of barely entangled polymers solutions,[39] has similarly been explained by a reduction of intermolecular constraints and hence of the coupling parameter. In fact, in these cases the experimental data gave direct evidence of the decrease of n with diluent concentration.[38,39]

We also anticipate that the alleviation of the constraints on the junctions by elongation of the network in the Flory model will carry over when considering the junction dynamics. If this is indeed the case, then the coupling model predicts a decrease of n with extension. Care must be exercised here because, while the constraints on junction fluctuations in the direction of the extension are relevant for the mechanical response of stretched networks, other experimental probes of junction motions may emphasize other directions. Although it is clear that the junction fluctuations are extended in the stretch direction, the transverse size of this domain is found to be essentially invariant to extension.[37,40] An analogue of the expected decrease of n with elongation of networks has been found in polycarbonate, an amorphous polymer, subjected to large deformation. After the polymer has been stressed beyond its yield point, the highly oriented chains in the yielded region were found[41] to exhibit a weaker degree of intermolecular cooperativity for local segmental motion. The segmental relaxation time, τ^*, and the coupling parameter, n, appearing in eq 9 decreased in comparison to the undeformed polycarbonate.[41]

The results of these comparisons of the Flory and the coupling models are summarized in Table 1. In the next section we cite experimental data on the relaxation dynamics of network junctions which confirm the expected variation of the coupling model parameters with the network characteristics.

Comparison with Experimental Results. The relaxation dynamics of junctions in polymer networks have not been well-known until recent solid-state ^{31}P NMR spin–lattice relaxation measurements in a series of poly(tetrahydrofuran) networks with tris(4-isocyanatophenyl)thiophosphate junctions.[30] The junction relaxation properties were studied in networks with molecular weights between cross-links, M_c, ranging from 250 to 2900. The dominant mechanism for ^{31}P nuclear spin relaxation was identified to be chemical shift anisotropy. The spin–lattice relaxation times measured over a wide range of temperatures were fitted satisfactorily by spectral density functions, $J(\omega)$, derived from the appropriate Fourier transforms of the stretched exponential correlation function given previously (eq 9), with τ^* assumed to have the Arrhenius temperature dependence of eq 11. From these fits Shi et al.[30] obtained the coupling parameter n, the apparent preexponential factor τ^*, and the apparent activation energy E_a^* for the networks of different cross-link densities, as well as for a swollen sample. The coupling model was actually employed to interpret their experimental data,[30] with n found to increase with decreasing molecular weight between cross-links and, at constant cross-link density, to decrease with the addition of diluent. These results are in accord with expectations based on the coupling model (see Table 1).

The apparent activation energy E_a^* is also found to increase significantly with higher cross-link density and, at constant cross-link density, to decrease with the addition of diluent. The product $(1 - n)E_a^*$ from all samples is remarkably constant. The constancy of this quantity is predicted by the coupling model, in that the product is the true microscopic energy barrier, E_a, independent of cross-link density and dilution.

The experimental determinations[30] for n, E_a^*, and the product $E_a = (1 - n)E_a^*$ are replotted versus M_c in Figures 1 and 2. It is evident from these plots that the ^{31}P NMR data of junction relaxation dynamics are in accord with the coupling model, as Shi et al. indicated in their paper. They also found that the apparent preexponential, τ_∞^*, decreases dramatically with higher cross-link density, as depicted in Figure 3. This behavior follows from the second relation (eqs 10 and 12) of the coupling model. As discussed above (Table 1), the coupling parameter increases with cross-link density (see Figure 1). From the expression for τ^* given by eq 12 or eq 14 and using the order of magnitude estimates for τ_∞ and t_c^{-1} given above, the experimentally observed dramatic increase of τ^* with cross-link density (Figure 3) is also anticipated from the coupling model. Using the reasonable but arbitrary choice of $\tau_\infty = 10^{-14}$ s and either $t_c = 5 \times 10^{-12}$ s or 2.5×10^{-12} s, together with the experimentally determined values of n as a function of M_c, eq 12 enables us to calculate τ_∞^* as a function of M_c. The agreement between the calculated values and the experimental results can be seen in Figure 3. The general agreement between the coupling model and the ^{31}P NMR data, concerning the dependencies of n, E_a^*, and τ_∞^* on network characteristics, is summarized in Table 1.

Summary

Experimental studies of elastomers have generally focused more on their equilibrium mechanical behavior than on the network dynamics per se. However, advanced NMR techniques, as illustrated by ^{31}P NMR spectroscopy,[30] as well as the neutron spin-echo experiments,[20]

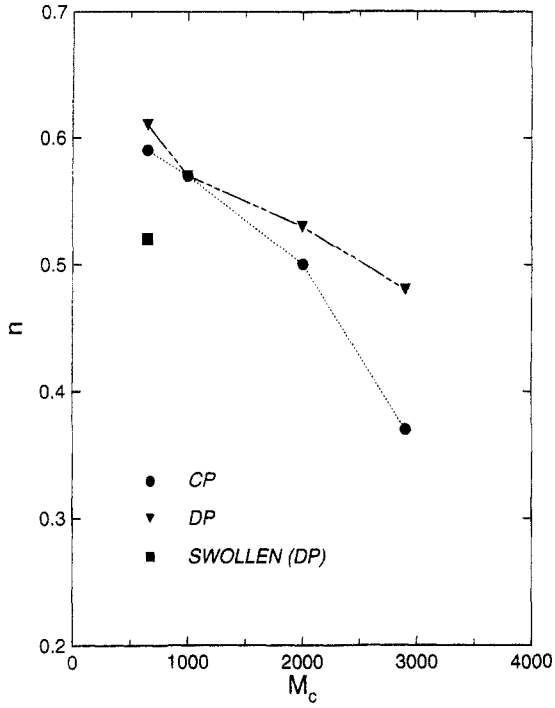

Figure 1. Plot of the coupling parameter of junction dynamics, n, determined by Shi et al. from their experimental data[30] for four polymer networks with different molecular weights between cross-links, M_c. Filled circles and filled inverted triangles are from ^{31}P NMR data taken using cross (CP) and direct (DP) polarizations, respectively. The filled square is data for a swollen sample with $M_c = 650$. The lines are drawn to guide the eyes.

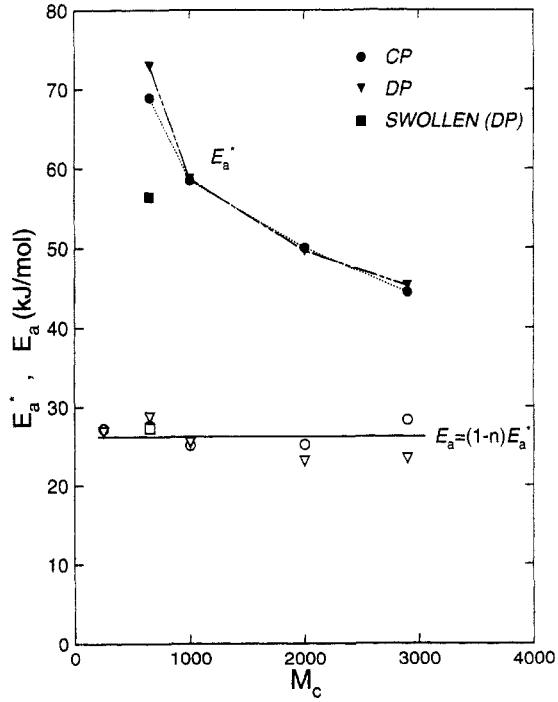

Figure 2. Filled symbols indicate the apparent activation enthalpy, E_a^*, determined by Shi et al.[30] from their ^{31}P NMR data. The corresponding unfilled symbols are the products $E_a = (1 - n)E_a^*$ formed by multiplying E_a^* in this figure with one minus the coupling parameter for the same network polymer given in Figure 1. Note that E_a is nearly constant, reflecting the true conformational energy barrier of the junction dynamics.

represent pioneering efforts to approach the study of networks in a more comprehensive fashion. Necessarily, theoretical treatments must in turn explicitly consider the junction dynamics. The development of the coupling model of relaxation described herein is an effort toward that end. Although its predictions concerning the behavior

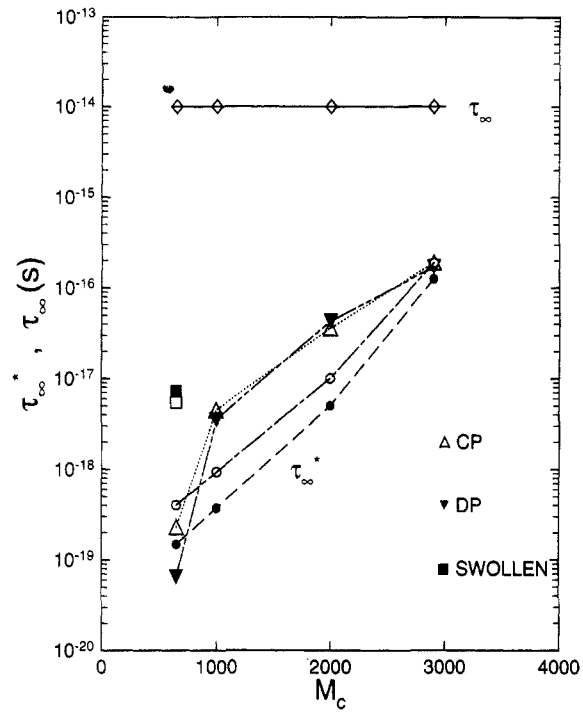

Figure 3. Unfilled triangles and filled inverted triangles are the apparent preexponential, τ_∞^*, determined by Shi et al. from their experimental data[30] for the four polymer networks by cross and direct polarizations, respectively. The filled square is τ_∞^* for the swollen polymer network with $M_c = 650$. Open diamonds and the solid line through them indicate that we have assumed arbitrarily that the real preexponential has the value of 10^{-14} s independent of M_c and diluent concentration. With this value of τ_∞ and the values of the coupling parameters given in Figure 1, τ_∞^* calculated from eq 12 are indicated by filled circles for the choice of $t_c = 4 \times 10^{-11}$ s and the unfilled circles for $t_c = 2 \times 10^{-11}$ s. The unfilled square is the value of τ_∞^* calculated for the swollen network polymer with $t_c = 4 \times 10^{-11}$ s.

of networks are plausible and in agreement with the ^{31}P NMR results, clearly much work remains to be done to elucidate the connection between junction dynamics and the elastic properties of networks.

Acknowledgment. This work was supported by the Office of Naval Research, KLN in part by contract N0001494WX23010.

References and Notes

(1) Treloar, L. R. G. *Rep. Prog. Phys.* **1973**, *36*, 755.
(2) James, H. M.; Guth, E. *J. Chem. Phys.* **1947**, *15*, 669.
(3) Treloar, L. R. G. *The Physics of Rubber Elasticity*; Clarendon: Oxford, U.K., 1975.
(4) Ronca, G.; Allegra, G. *J. Chem. Phys.* **1975**, *63*, 4990.
(5) Flory, P. J. *Proc. R. Soc. London A* **1976**, *351*, 351.
(6) Flory, P. J. *Polym. J.* **1985**, *17*, 1.
(7) Flory, P. J. *Rubber Chem. Technol.* **1979**, *52*, 110.
(8) Flory, P. J.; Erman, B. *Macromolecules* **1982**, *15*, 800, 806.
(9) Erman, B.; Flory, P. J. *J. Chem. Phys.* **1978**, *68*, 5363.
(10) Duering, E. R.; Kremer, K.; Grest, G. S. *Phys. Rev. Lett.* **1991**, *67*, 3531; *Macromolecules* **1993**, *26*, 3241.
(11) Vilgis, T. A.; Boue, F. *J. Polym. Sci.* **1988**, *26*, 2291.
(12) Grosberg, A. *Macromolecules* **1993**, *26*, 3200.
(13) Marrucci, G. *Macromolecules* **1981**, *14*, 434.
(14) Gaylord, R. J. *Polym. Bull.* **1982**, *8*, 325; **1983**, *9*, 181.
(15) Ball, R. C.; Doi, M.; Edwards, S. F.; Warner, M. *Polymer* **1981**, *22*, 1010.
(16) Adolf, M. *Macromolecules* **1987**, *20*, 116; **1988**, *21*, 2249.
(17) Beltzung, M.; Picot, C.; Herz, J. *Macromolecules* **1984**, *17*, 663.
(18) Ullmann, B. *Macromolecules* **1982**, *15*, 582.
(19) Erman, B.; Monnerie, L. *Macromolecules* **1989**, *22*, 3342; **1992**, *25*, 4456.
(20) Oeser, R.; Ewen, B.; Richter, D.; Farago, B. *Phys. Rev. Lett.* **1988**, *60*, 1041.

(21) Ngai, K. L.; White, C. T. *Phys. Rev.* **1980**, *B20*, 2475. Ngai, K. L. *Comments Solid State Phys.* **1979**, *9*, 121. Ngai, K. L.; Peng, S. L.; Tsang, K. Y. *Physica A* **1992**, *191*, 523, Tsang, K. Y.; Ngai, K. L., to be published.
(22) Ngai, K. L.; Rajagopal, A. K.; Teitler, S. *J. Chem. Phys.* **1988**, *88*, 5086.
(23) Ngai, K. L.; Rendell, R. W.; Rajagopal, A. K.; Teitler, S. *Ann. New York Acad. Sci.* **1986**, *484*, 150.
(24) Ngai, K. L.; Rendell, R. W.; Yee, A. F.; Plazek, D. J. *Macromolecules* **1991**, *24*, 61.
(25) See recent review: Ngai, K. L. In *Disorder Effects on Relaxation Processes*; Blumen, A., Richert, R., Eds.; Springer-Verlag: New York, 1994; Chapter 4.
(26) Ngai, K. L. *J. Chem. Phys.* **1993**, *98*, 6.
(27) Colmenero, J.; Arbe, A.; Alegria, A. *Phys. Rev. Lett.* **1993**, *71*, 2603.
(28) Roe, R.-J. *J. Chem. Phys.* **1993**.
(29) For examples, see: Plazek, D. J.; Zheng, X. D.; Ngai, K. L. *Macromolecules* **1992**, *25*, 4920. Ngai, K. L.; Plazek, D. J.; Bero, C. *Macromolecules* **1993**, *26*, 1065.
(30) Shi, J.-F.; Dickinson, L. C.; MacKnight, W. J.; Chien, J. C. W. *Macromolecules* **1993**, *26*, 5908.
(31) Bernard, W.; Callen, H. B. *Rev. Mod. Phys.* **1959**, *31*, 1017.
(32) Sanjuan, J.; Llorente, M. A. *J. Polym. Sci., Polym. Phys. Ed.* **1988**, *26*, 235.
(33) Allen, G.; Kirkham, M. J.; Padget, J.; Price, C. *Trans. Faraday Soc.* **1971**, *67*, 1278.
(34) Mark, J. E. *Rubber Chem. Technol.* **1975**, *48*, 495.
(35) Brontzman, R. W.; Mark, J. E. *Macromolecules* **1986**, *19*, 667.
(36) Erman, B.; Kloczkowski, A.; Mark, J. E. *Macromolecules* **1989**, *22*, 1432.
(37) Adolf, D. B.; Curro, J. G. *Macromolecules* **1987**, *20*, 1646.
(38) Ngai, K. L. *Macromolecules* **1991**, *24*, 4865.
(39) Ngai, K. L.; Rendell, R. W. *Macromolecules* **1987**, *20*, 1066.
(40) Flory, P. J. *Macromolecules* **1975**, *63*, 4990.
(41) Ngai, K. L.; Roland, C. M.; Yee, A. F. *Rubber Chem. Technol.* **1993**, *66*, 615.
(42) Flory, P. J.; Erman, B. J. *J. Polym. Sci., Polym. Phys. Ed.* **1984**, *22*, 1953.